

# Enhancing the reliability of protection scheme for PV integrated microgrid by discriminating between array faults and symmetrical line faults using sparse auto encoder

ISSN 1752-1416

Received on 20th March 2018

Revised 20th September 2018

Accepted on 26th October 2018

E-First on 26th November 2018

doi: 10.1049/iet-rpg.2018.5627

www.ietdl.org

Murli Manohar<sup>1</sup>, Ebha Koley<sup>1</sup>, Subhojit Ghosh<sup>1</sup> <sup>1</sup>Department of Electrical Engineering, National Institute of Technology, Raipur (C.G.), India

✉ E-mail: sghosh.ele@nitrr.ac.in

**Abstract:** The ever increasing power demand and stress on reducing carbon footprint have paved the way for widespread use of photovoltaic (PV) integrated microgrid. However, the development of a reliable protection scheme for PV integrated microgrid is challenging because of the similar voltage-current profile of PV array faults and symmetrical line faults. Conventional protection schemes based on pre-defined threshold setting are not able to distinguish between PV array and symmetrical faults, and hence fail to provide separate controlling actions for the two cases. In this regard, a protection scheme based on sparse autoencoder (SAE) and deep neural network has been proposed to discriminate between array faults and symmetrical line faults in addition to perform mode detection, fault detection, classification and section identification. The voltage-current signals retrieved from relaying buses are converted into grey-scale images and further fed as input to the SAE to perform unsupervised feature learning. The performance of the proposed scheme has been evaluated through reliability analysis and compared with artificial neural network, support vector machine and decision tree based techniques under both islanding and grid-connected mode of the microgrid. The scheme has been also validated for field applications by performing real-time simulations on OPAL-RT digital simulator.

## 1 Introduction

The commitment toward the reduction of greenhouse gas emission has prompted increased penetration of renewable resources in the small and medium distribution networks to ensure reliable and continuous power supply with superior power quality [1]. Power system network involving interconnection of multiple low rating renewable and/or conventional sources is commonly referred to as microgrid [2]. Among the commonly used renewable distributed energy resources (DERs) in a microgrid, the integration of photovoltaic (PV)-based generation has gained significant importance due to ease of availability of solar energy and economic operation [3]. In spite of the wide penetration, the intermittent and irregular operating nature of PV because of its dependence on environmental conditions has posed serious protection challenges for PV integrated microgrids. The disparity in operating characteristics of PV and other DERs and divergent variation in current–voltage profile post-fault under dual operating modes (islanding and grid connected) of the microgrid demand resilience in the event of shunt faults in the distribution lines.

In addition to the line faults, the other common disturbance which affects the operation of a microgrid is faults in the PV array. Although both symmetrical line faults and PV array faults are contingencies, from which the microgrid needs to be protected, the control actions required for the fault cases are different, i.e. in case of symmetrical fault, the relaying action aims at isolating the faulty feeder, whereas the occurrence of PV array fault demands disconnection of faulty source only. However, the conventional relays, which are programmed to operate on the current–voltage information, quite often are unable to discriminate between faults on the array and distribution line fault leading to nuisance tripping and possible power outage. This is attributed to the similar current–voltage profile resulting from the two scenarios.

With regard to protection issues in PV integrated microgrids, a large number of techniques have been proposed during the last few years. Some of the significant techniques among them include discrete wavelet transform (DWT) and decision tree (DT)-based approach [4], superimposed reactive energy calculation using Hilbert transform [5], time–frequency transform-based differential

scheme to obtain the relay threshold setting [6], voltage magnitude and angle-based classification scheme [7], fast recursive discrete Fourier transform (DFT) and fuzzy logic-based decision-making module for relay current setting [8], DWT and ensemble classifier-based scheme [9], DER impedance calculation-based technique [10] and differential current-based adaptive thresholding [11]. These techniques though validated for different fault scenarios in the microgrid, none of them have been evaluated with regard to their ability in discriminating between the array and line faults. On the other hand, techniques have been reported for detecting and classifying array faults [12–14] but all the schemes have been proposed for standalone PV systems and not extended for microgrids.

From the literature review carried out regarding the protection of PV integrated microgrids and isolated PV systems, it can be concluded that the proposed techniques have concentrated on either line faults or array faults only. None of the reported schemes can detect and discriminate both the faults simultaneously. In this regard, the present work proposes a microgrid protection technique, which in addition to perform the intended task of fault detection, classification and section identification of line faults, is also able to detect the array faults and avoids nuisance tripping arising due to array faults.

In recent times, various computational intelligence techniques such as support vector machine (SVM) [15], DT [4] and fuzzy logic [16] have been adopted for detection and classification of faults in power system. The appropriateness of a computational intelligence-based protection scheme is heavily dependent on the effectiveness of the feature extraction technique and classification approach. The feature extraction process plays a significant role in preserving the contextual and discriminatory information extracted from the original signals. The feature extraction techniques adopted in microgrid protection can be broadly classified as time domain, frequency domain and combined time–frequency domain. Some of the significantly reported protection schemes use DFT [8, 17], DWT [4], Hilbert–Huang transform [18] and S-transform [6] for feature extraction. The extraction of useful and discriminatory features from domain transformation demands necessary pre-

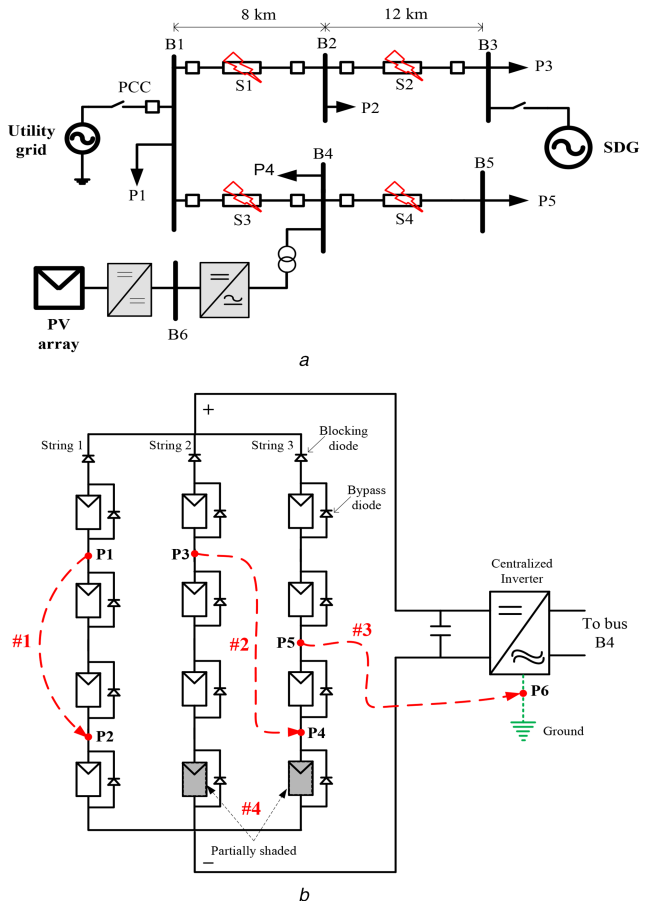


**Fig. 1** Schematic diagram of

(a) Microgrid system under study, (b) PV array with marked fault locations

processing for noise removal, dimensionality reduction and removing redundant information, which increases the computational cost, especially for large datasets. To overcome the above difficulty, the present work proposes a stacked sparse autoencoder (SAE)-based deep neural network (DNN) scheme which has the ability to automatically learn features from the unlabelled dataset consisting of instantaneous values of voltage and current signals without specifically extracting attributes for different fault cases [19, 20]. Owing to the effective performance of SAE in discovering the system structure information from input dataset with reduced computation effort, it has been successfully implemented in various classification applications [21–23].

However, to the best of our knowledge, SAE has not been applied for microgrid protection. In the present work, a scheme based on the combined framework of SAE and DNN has been adopted to perform mode detection, fault detection, classification and section identification. In addition to this, as mentioned earlier, the scheme possesses selectiveness in performing the desired to relay action irrespective of the similar behaviour of the DER (PV array) fault and distribution line faults. The novelty of the proposed work can be summarised as:

- Design and development of a reliable protection scheme for PV integrated microgrid, which can discriminate between symmetrical distribution line faults and PV array faults.
- Development of SAE-DNN-based protection scheme to perform fault detection, classification and section identification in the distribution system under both operating modes of the microgrid.
- Detection of PV array faults using the voltage-current information on the AC side.
- Real-time validation of the proposed scheme on the OPAL-RT digital simulator.

Rest of this paper is organised as follows: Section 2 briefly describes the microgrid system considered under study. The

detailed explanation of the development of SAE-based protection scheme is included in Section 3. Section 4 presents the performance evaluation results with concluding remarks in Section 5.

## 2 Microgrid system under study

The layout of 34.5 kV, 60 Hz balanced microgrid system [7] adopted in the present work has been depicted in Fig. 1a. The utility grid is connected to the microgrid through a switch at the point of common coupling, which facilitates the transition between grid-connected and islanded mode operation. Two DERs including synchronous (synchronous diesel generator (SDG)) and inverter interfaced (PV) are connected into the microgrid distribution network at buses B3 and B4, respectively. The bi-directional power exchange takes place during the grid-connected mode with SDG disconnected, whereas during the islanding mode, both DERs feed the loads. The microgrid distribution line is constituted by four Sections S1, S2, S3 and S4 with pairs S1, S2 and S3, S4 representing the two parallel zones of line, spread over a line length of 20 km. The loads are represented by P1, P2, P3, P4 and P5. Fault scenarios including the distribution line faults and PV array faults have been simulated under both modes of operations.

To analyse the impact of PV array faults on the distribution network, the PV source at bus B4 has been modelled as distributed series-parallel combination of PV modules with three parallel strings each consisting of four modules in series as shown in Fig. 1b. A blocking diode is connected in series with each parallel string to prevent the flow of back-feed current and each module consists of a bypass diode connected in anti-parallel to prevent hotspot during partial shading conditions [24]. Four different fault situations in PV array involving line-line (LL) fault within same string, LL fault among parallel strings, line-ground (LG) fault and partial shading have been created at marked locations #1, #2, #3 and #4, respectively. However, the marked fault locations are arbitrary and may occur within any two suitable points of the array.

## 3 Proposed protection methodology

As described in Section 1, the similar behaviour (current profile) of PV array faults at DER side and three-phase symmetrical faults at distribution network side demand a relaying scheme which should be able to discriminate between the two situations to avoid nuisance tripping of the relay during both operating modes. To perform the tasks of mode detection, fault detection, classification and faulty section/zone identification, the following fault scenarios have been simulated in two phases for each operating mode of the microgrid:

- Simulation of shunt faults including LG, LL, line to line to ground (LLG), line to line to line (LLL) and line to line to line to ground (LLLG) is carried out in each of the four sections Sections S1, S2, S3 and S4 of the line with variation in fault parameters such as fault resistance, inception angle and location.
- PV array faults involving LG, LL and partial shading are created in the array for which, one case corresponding to each kind has been marked in Fig. 1b.

To depict the close resemblance in the current profile between PV array fault and three-phase symmetrical fault in the line, the three-phase current waveform at bus B4 during a ground fault in PV array and LLLG fault in Section S4 with fault resistance,  $R_f = 50 \Omega$  at  $t = 0.3$  s is shown in Figs. 2a and b, respectively. It can be observed that both the two scenarios result in a similar current profile. Similarly, other PV faults described in the preceding section also bear similar profile with the symmetrical faults in the distribution lines.

### 3.1 DNN architecture using SAE

The development of an effective and reliable protection scheme is heavily dependent on the extraction of discriminative attributes for different scenarios. The selection of a technique for extracting

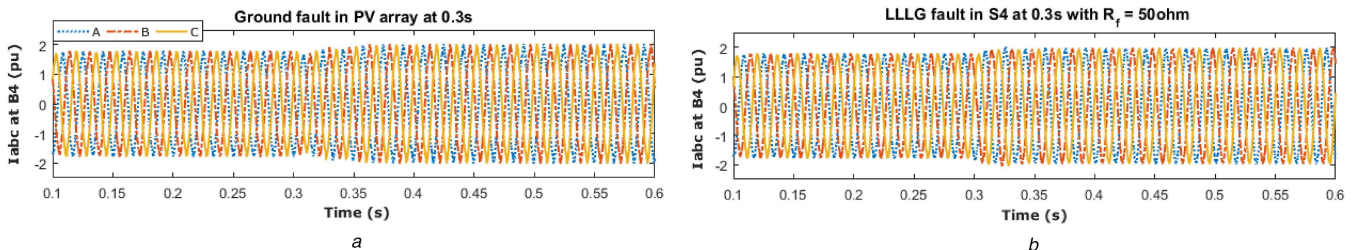


**Fig. 2**  $I_{abc}$  at bus B4 during

(a) Ground fault in PV array, (b) LLLG fault in Section S4 at  $R_f = 50 \Omega$

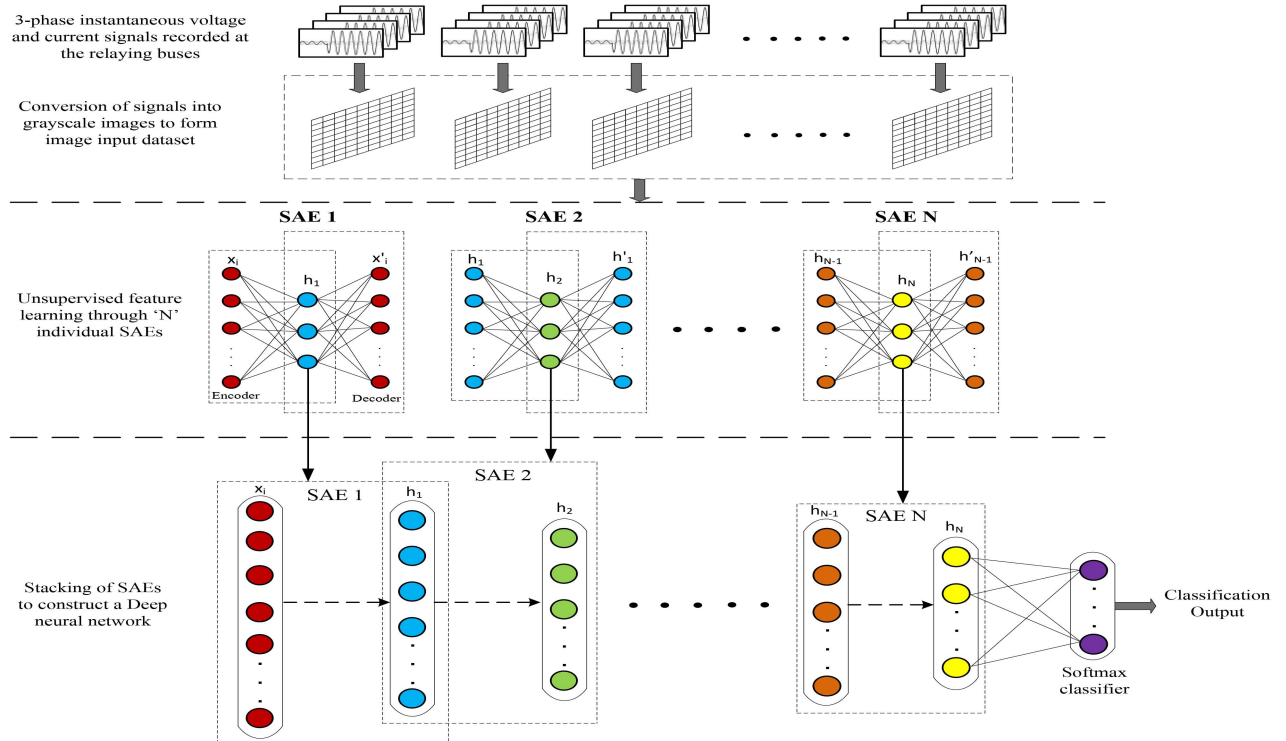


**Fig. 3** Structure of SAE-based DNN

features from time-domain signals are heavily realised on the dataset characteristics. For the majority of the artificial intelligence-based protection schemes, the major component of computational cost is attributed to the complexity of the feature extraction technique. Also, for complex datasets with non-linearity and a redundant information extracting useful information for simpler representation of the scenario is always a challenge. Inspired by these limitations of conventional protections schemes, an SAE-based DNN has been used to develop the protection scheme for the microgrid. The SAE-based scheme facilitates unsupervised learning without labelling of individual data points and does not involve the transformation of the data from one domain to another, which reduces the computational cost and makes it suitable for handling larger datasets [25]. The structure of the SAE-DNN-based classification approach is depicted in Fig. 3.

An autoencoder neural network consisting of three layers, namely input, hidden and output layers, in which the input and hidden layers form the encoder network and hidden and output layers form the decoder network. The encoder performs the conversion of input vectors into the hidden representation codes, whereas the reconstruction of original input from the learned hidden codes is carried out by the decoder. The feature learning of input vectors is carried out in an unsupervised manner with the aim of minimising reconstruction errors [26]. In SAE, a sparsity penalty constraint is added to the cost function of autoencoder, which helps in learning of more representative features of the input than an autoencoder.

For an input vector  $\mathbf{x}^i$ , from the dataset  $\{\mathbf{x}^i\}_{i=1}^n$ , the representation vector,  $\mathbf{h}^i$  and the reconstructed vector,  $\mathbf{x}'^i$  can be written as

$$\mathbf{h}^i = f(W^{(1)}\mathbf{x}^i + b^{(1)}) \quad (1)$$

$$\mathbf{x}'^i = f(W^{(2)}\mathbf{h}^i + b^{(2)}) \quad (2)$$

where  $W^{(1)}$ ,  $W^{(2)}$  are the weights and  $b^{(1)}$  and  $b^{(2)}$  are the bias vectors and  $f$  is the activation function. The reconstruction error  $L(\mathbf{x}^i, \mathbf{x}'^i)$  between  $\mathbf{x}^i$  and  $\mathbf{x}'^i$  can be represented as

$$L(\mathbf{x}^i, \mathbf{x}'^i) = \frac{1}{2} \mathbf{x}^i - \mathbf{x}'^i \quad (3)$$

$$J(W, b) = \left[ \frac{1}{n} \sum_{i=1}^n L(\mathbf{x}^i, \mathbf{x}'^i) \right] + \frac{\lambda}{2} \sum_{l=1}^{m_l-1} \sum_{k=1}^{S_l} \sum_{j=1}^{S_{l+1}} (W_{jk}^{(l)})^2 \quad (4)$$

The first term in the above expression represents the reconstruction error of the whole dataset and the second term denotes the regularisation weight. The term  $\lambda$  denotes the weight decay parameter,  $m_l$  represents the layer number in the network,  $S_l$  represents the neurone number in the  $l$ th layer with  $W_{jk}^{(l)}$  defining the weight between neurone  $k$  in the  $(l+1)$ th layer and neurone  $j$  in the  $l$ th layer.

After the addition of sparsity penalty term (4), it can be written as

$$J_{\text{sparse}}(W, b) = J(W, b) + \beta \sum_{g=1}^e \left( \rho \log \frac{\rho_g}{\rho'_g} + (1-\rho) \log \frac{1-\rho_g}{1-\rho'_g} \right) \quad (5)$$

where

$$\rho'_g = \frac{1}{n} \sum_{i=1}^n h_g^i \quad (6)$$

Here,  $\rho'_g$  represents the average activation value of hidden unit  $g$  as defined in (6),  $\rho$  is the sparsity parameter and  $\beta$  is the sparsity penalty term parameter.

The primary objective of SAE is to perform the learning of sparse features by extracting information to the maximum extent possible from the input dataset and minimising the cost function  $J_{\text{sparse}}(W, b)$  using back propagation algorithm. The detailed procedure adopted for constructing and training the DNN using stacked SAEs is detailed below (Fig. 4):

- (i) The voltage and current signals retrieved from the relaying buses B1 and B4 (Fig. 1a) are converted to grey-scale images to form the input dataset with each image set representing a particular case. The acquired dataset of input vectors forms the unlabelled training set,  $x_{\text{train}} = \{x^i\}_{i=1}^n$ .
- (ii) Unsupervised feature learning of ' $N$ ' individual SAEs is carried out using the unlabelled training set obtained in step 1 in such a manner that the coding vector obtained at the hidden layer of the preceding SAE becomes the input layer for the next SAE.
- (iii) Followed by individual training, the SAEs are stacked to form a DNN containing the multiple hidden layers of  $N$  number of SAEs. The weights of the DNN are initialised by pre-training of SAEs one by one. Furthermore, the DNN is fine-tuned using backpropagation algorithm to improve the performance.
- (iv) In this step, the supervised fine-tuning is performed. The softmax classifier is trained using the hidden activities of  $N$ th SAE to perform the classification task with assigned target labels corresponding to the input dataset. Finally fine-tuning of DNN is performed to obtain improved classification accuracy.
- (v) With the trained DNN, testing is performed to predict the classification output. On the basis of the actual testing target and predicted target values, classification accuracy is calculated.

### 3.2 Development of the proposed protection scheme

The overall functioning of the SAE–DNN-based protection scheme has been described in the form of a flowchart depicted in Fig. 5. The instantaneous voltage and current signals recorded at the relaying buses are converted into image dataset to be fed as input to the SAE–DNN-based protection scheme. Separate modules have been developed to perform the tasks of mode detection, fault detection, classification and section identification. The fault analysis has been carried out under both operating modes of the microgrid, i.e. islanding and grid connected. Different cases of line faults have been simulated in each section of the distribution line with wide variation in fault parameters including fault resistance  $R_f$  ( $0\text{--}100\ \Omega$ ), inception angle  $\theta$  ( $0^\circ\text{--}90^\circ$ ) and location  $L_f$  ( $0\text{--}20\text{ km}$ ). Similarly, the dataset for PV array faults has been generated by considering the different configurations of LG faults, LL faults and partial shading in the array involving different PV modules.

Quite often PV array faults generate arcs in the array. For the present system, the arc faults in PV array have an insignificant effect on the voltage–current profile at the far-end buses, i.e. B1 and B4. However, the post-fault variation in current and voltage at the near-end PV bus, i.e. B6 is significant. Hence, providing the necessary protection against arc faults using the proposed scheme demands inclusion of voltage–current data recorded at B6 for

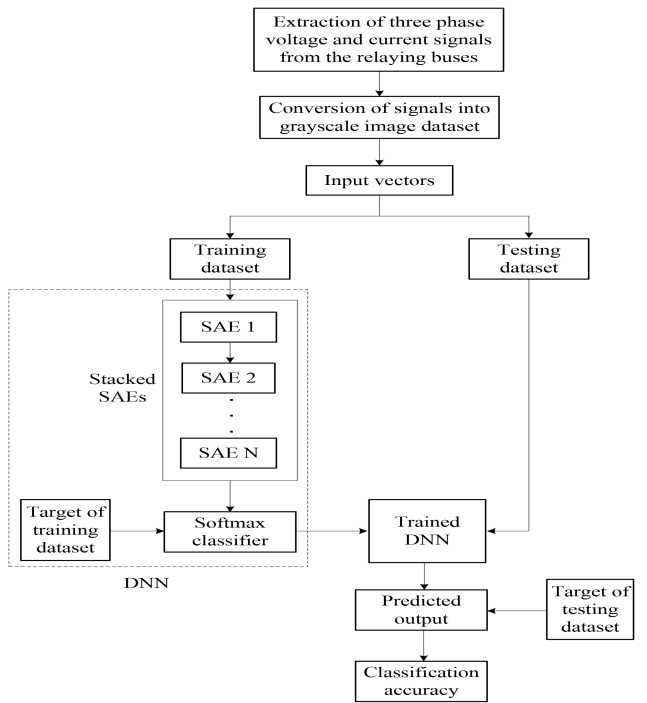


**Fig. 4** Flowchart of the proposed SAE-based classification module

training the proposed SAE–DNN algorithm. In this regard, different arc faults have been simulated and included in the input training dataset. The SAE–DNN re-trained with the updated dataset is able to detect the arc fault cases.

The no-fault (NF) cases have been generated by considering variation in the loading condition. The details of the training and testing dataset are mentioned in Table 1.

**3.2.1 Mode detection module:** The wide disparity in voltage–current profile during islanding and grid-connected mode of the microgrid demands separate protection strategy for both the cases. Thus, before applying a particular protection strategy, it is a prerequisite to detect the operating mode of the microgrid. To perform this task, an SAE–DNN-based mode detection module (M1) is developed with two targets, namely ‘GC’ and ‘IM’.

**3.2.2 Fault detection, classification and section identification modules:** Depending on the output received by the mode detection module M1, the protection strategy corresponding to the selected mode is triggered to perform the fault detection, classification and section identification tasks simultaneously. Modules M2 and M5 are dedicated to perform the fault detection task in grid-connected and islanding mode, respectively, to detect the line fault and PV array fault. In case the line fault is detected, the fault classification and section identification tasks are performed simultaneously by the modules M4 and M3, respectively, in grid-connected mode and M6 and M7, respectively, in islanding mode. For both the modules developed for classification task (M4 and M6), the classification involves selection from 11 possible fault types, i.e. phase A to ground (AG), phase B to ground (BG), phase C to ground (CG), phase A to phase B (AB), phase A to phase C (AC), phase B to phase C (BC), phase A to phase B to ground (ABG), phase A to phase C to ground (ACG), phase B to phase C to ground (BCG), phase A to phase B to phase C (ABC), phase A to phase B to phase C to ground (ABCG) and NF case. It is worth mentioning that the NF cases have been simulated considering the variation in loading condition. Further following the mode detection, M3 and M6 modules identify the faulty section of the distribution line. The section identifier is designed to accommodate four possible target outputs, namely S1, S2, S3 and S4.

As stated earlier, different relaying actions are required for PV array faults and distribution line faults. Hence, in case a PV array fault is detected, the faulty PV source is disconnected, whereas in case of line faults, depending on the information obtained

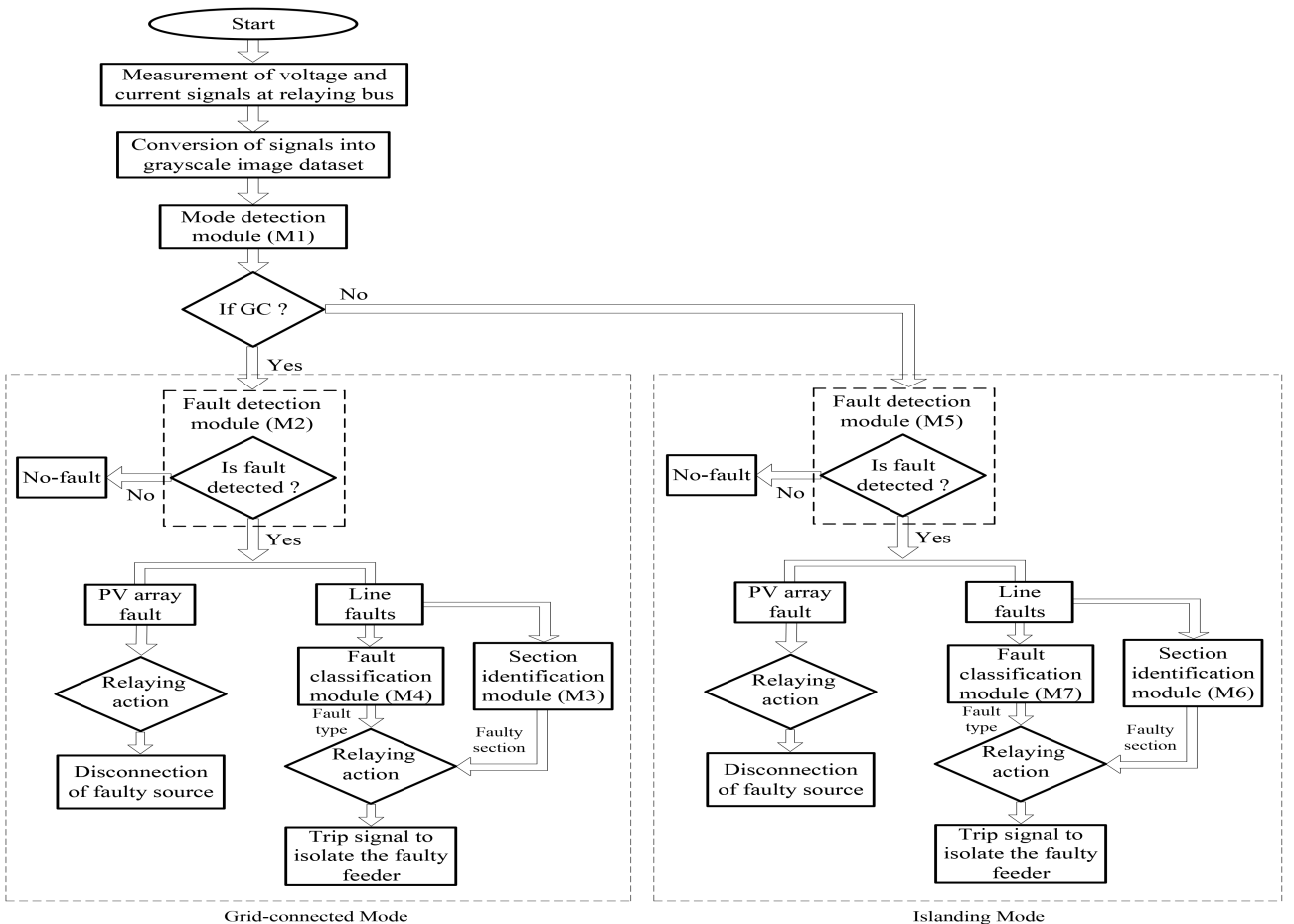


Fig. 5 Flowchart of proposed protection scheme

Table 1 Number of training and testing cases

Number of cases	Fault cases					NF cases	
	Line faults					PV array faults	NF cases
	LG	LL	LLG	LLL	LLLG		
training	1916	638	1916	214	638	180	140
testing	820	274	820	92	274	76	60

regarding the type of fault and faulty section, the relay generates the trip signal for the isolation of faulty feeder as shown in the flowchart (Fig. 5).

#### 4 Performance evaluation of the proposed protection scheme

The effectiveness of the proposed SAE-DNN-based protection scheme in performing the tasks of fault detection, classification and section identification for both operating modes has been evaluated in this section. In this regard, different cases involving all types of faults (distribution line and PV array faults) with variation in fault parameters and disturbance situations such as variation in loading condition have been simulated to generate the testing dataset (Table 1). Post-training, the performance of different modules in performing the intended tasks has been analysed. The classification accuracy of the proposed SAE-DNN-based technique has been compared with DT, SVM and artificial neural network (ANN)-based techniques for varying fault cases in Fig. 6.

The higher classification accuracy obtained through SAE-DNN-based scheme validates the effectiveness of the proposed scheme. Furthermore, the performance of different modules of the proposed scheme is detailed in the following sections.

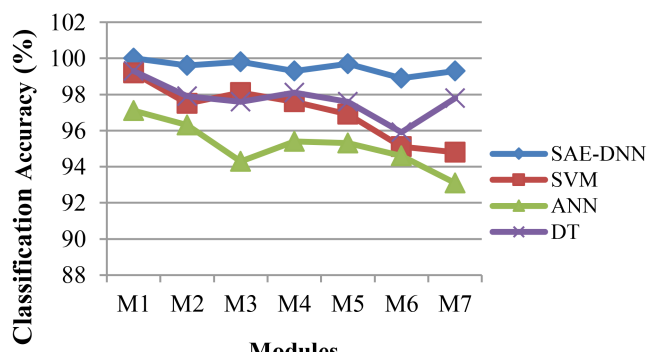


Fig. 6 Comparison of classification accuracies (%) obtained by SAE-DNN with SVM, ANN and DT-based schemes

##### 4.1 Mode detection

A total number of 4029 cases consisting of 2821 training and 1208 testing cases in each mode have been generated to perform the mode detection task. The task of detecting the transition between grid-connected and islanding mode operation of microgrid has been effectively performed by the SAE-DNN-based mode detector M1 with 100% classification accuracy. While the DT, SVM and ANN-based classification modules could attain accuracies of 99.3, 99.2 and 97.1%, respectively.

**Table 2** Reliability analysis of fault detection and classification techniques in both operating modes

Techniques	Mode of operation			
	Grid connected		Islanding	
	Dependability, %	Security, %	Dependability, %	Security, %
SAE-DNN	99.92	100.00	99.83	98.33
DT	98.05	96.67	97.88	93.33
SVM	97.79	95.00	97.54	91.67
ANN	96.09	91.67	95.75	85.00

**Table 3** Mode-wise performance comparison of the proposed section identification technique with other techniques

Mode of operation	Sections	Testing accuracy, %			
		SAE-DNN	DT	SVM	ANN
Grid connected	S1	99.56	97.33	97.78	96.44
	S2	100.00	97.97	97.10	94.49
	S3	99.56	97.78	96.89	94.67
	S4	99.71	97.68	96.52	92.46
Islanding	S1	98.67	96.00	95.56	92.89
	S2	99.13	96.52	95.94	91.30
	S3	99.11	96.00	94.67	93.33
	S4	98.55	95.36	94.49	91.88

#### 4.2 Fault detection and classification

The test dataset for fault detector consists of 1208 cases (1140 line faults, 38 PV array faults and 30 NF cases). The testing dataset of 1140 distribution line fault cases for each mode has been used to examine the performances of M4 and M7. The reliability is an important factor in evaluating the protection scheme. Thus to verify reliability, different faults with variation in fault parameters including fault resistance, inception angle and location, NF cases and PV array fault cases are considered. The reliability assessment of the proposed SAE-DNN-based fault detector and classifier has been carried out and compared with DT, SVM and ANN-based schemes in terms of the following statistical measures:

- (i) **Dependability**: It refers to possible misdetection of fault and is estimated as the percentage of the total number of correctly predicted fault cases to that of the total number of actual fault cases.
- (ii) **Security**: It refers to the possibility of generating false alarms and is expressed as the percentage of the total number of NF situations correctly predicted to that of the total number of actual NF cases.

Furthermore, the comparison of the proposed SAE-DNN-based fault detector and classifier has been carried out with DT, SVM and ANN-based techniques in terms of reliability indices in Table 2. It can be observed that for the same testing dataset, the proposed fault detection and classification module achieves a higher degree of dependability and security in both operating modes of microgrid as compared with the other two techniques.

#### 4.3 Section identification

In this section, the testing accuracy of the proposed section identification modules in both modes has been compared with DT, SVM and ANN-based techniques and the results have been summarised in Table 3. The obtained results indicate that the proposed SAE-DNN-based section identifier outperforms the other two methods with an overall accuracy of 99.70 and 98.86% in grid-connected and islanding modes, respectively.

To evaluate the appropriateness of the proposed scheme under grid-connected and islanding mode for the wide variation in fault current, a BG fault has been simulated in Section S3 at  $t = 0.4$  s with  $R_f = 1 \Omega$  and  $L_f = 1$  km. The current waveform and response of the proposed SAE-DNN-based algorithm during fault under each mode of operation is depicted in Figs. 7a–d. For both the cases, the fault is detected and correctly classified within one cycle, i.e. 8.8 and 12.8 ms for grid-connected and islanding modes, respectively.

#### 4.4 Performance of the proposed scheme against false tripping situations

The response of the proposed SAE-DNN-based scheme has been analysed against various random fault and NF situations involving PV array faults, distribution line faults and load variation. As discussed earlier, the similar behaviour of PV array faults and distribution line faults may create false tripping situations for conventional relaying schemes resulting in reduced security. Hence, the appropriateness of the proposed relaying scheme has been evaluated against random scenarios in both operating modes of the microgrid as mentioned in Table 4. From the obtained output, it can be inferred that the proposed scheme successfully performs the intended fault detection/classification task with a fast relaying action under both modes of operations.

The test results of the proposed relaying scheme against the fault situations described in Figs. 2a and b have been displayed in Figs. 8a and b, respectively. The relay operation times calculated from the instant of fault inception at  $t = 0.3$  s to the generation of a trip signal for the above two cases are 0.0146 and 0.0166 s, respectively. The relay operation time for all other fault cases has also been calculated in a similar manner and has been found in the range of 13.9–16.6 ms.

As per the performance analysis carried out in the present and preceding sections, it can be concluded that the proposed SAE-DNN-based scheme is fast and efficient in performing the tasks of fault detection, classification and section identification satisfactorily under both operating modes of the microgrid.

#### 4.5 Response of the proposed SAE-DNN scheme against high-impedance fault

The majority of microgrid protection schemes are not activated by the inadequate rise in current for faults occurring with high fault resistance at the far end of the distribution line. In this context, the performance of the proposed SAE-DNN scheme has been examined for faults with high fault resistance. Some of the test results for faults involving the high value of fault resistance have been summarised in Table 5. The response of the proposed scheme for each fault type against high fault resistance under both modes of operations (grid connected and islanding) clearly indicates its immunity against high fault resistance.

The energised conductors in the distribution line quite often come in contact to the ground surface through poor conducting materials such as asphalt, sand or trees which may lead to arcing. Such faults are high-impedance AC arc faults, which are dynamic in nature. The time-varying behaviour of high-impedance fault (HIF) has been modelled through the two-diode model [27] with

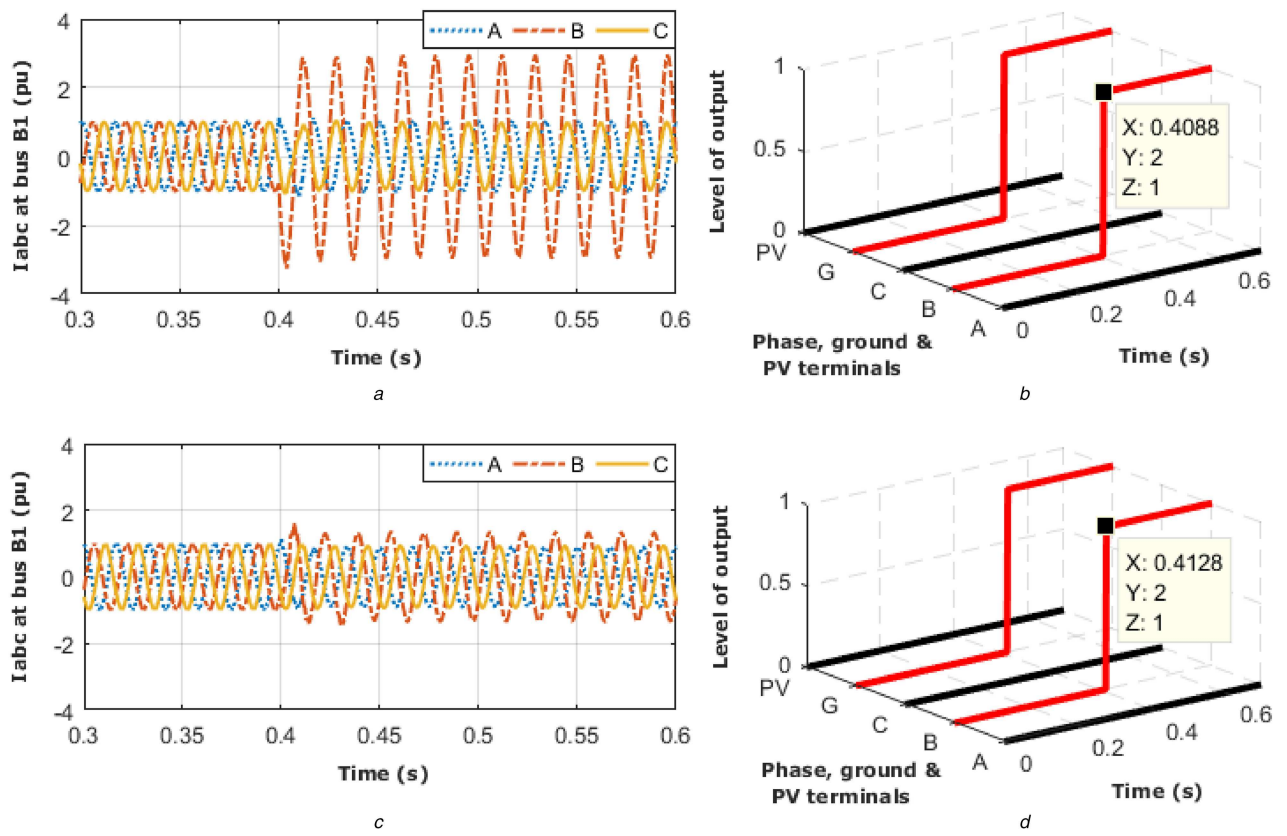


**Fig. 7** Response of the proposed SAE–DNN-based protection scheme for BG fault in Section S3 at  $t = 0.4$  s with  $R_f = 1\Omega$  and  $L_f = 1$  km

(a) Current waveform at bus B1 during grid-connected mode, (b) Response for grid-connected mode, (c) Current waveform at bus B1 during islanding mode, (d) Response for islanding mode

**Table 4** Response of SAE–DNN-based relaying scheme against random fault and NF situations

Situation	Parameters	Section	Fault detector/classifier output	Mode of operation			
				Grid connected	Relay operation time, s	Fault detector/classifier output	Islanding
fault situation	PV array fault	LG	Ext	PV fault	trip signal for PV disconnection	0.0146	PV fault
	PV array fault	LL	Ext	PV fault	trip signal for PV disconnection	0.0139	PV fault
	ABCG fault $R_f = 50\Omega$ , $\theta = 90^\circ$ , $L_f = 1$ km	S4	ABCG	trip signal to phases A, B, C and G	0.0164	ABCG	trip signal to phases A, B, C and G
	ABC fault $R_f = 0\Omega$ , $\theta = 0^\circ$ , $L_f = 5$ km	S3	ABC	trip signal to phases A, B and C	0.0159	ABC	trip signal to phases A, B and C
	ABG fault $R_f = 1\Omega$ , $\theta = 0^\circ$ , $L_f = 2$ km	S1	ABG	trip signal to phases A, B and G	0.0153	ABG	trip signal to phases A, B and G
	CG fault $R_f = 5\Omega$ , $\theta = 90^\circ$ , $L_f = 7$ km	S2	CG	trip signal to phases C and G	0.0149	CG	trip signal to phases C and G
	BC fault $R_f = 0\Omega$ , $\theta = 0^\circ$ , $L_f = 3$ km	S3	BC	trip signal to phases B and C	0.0162	BC	trip signal to phases B and C
NF situation	load variation + 20%	.....	NF	no action	.....	NF	no action
	load variation + 60%	.....	NF	no action	.....	NF	no action

wide variation in the fault parameters. The performance of the proposed SAE–DNN-based scheme has been examined against HIFs under both modes of operations of the microgrid. To exemplify the behaviour of HIF post-fault, an AG arc fault has been simulated in Section S3 at  $t = 0.45$  s in grid-connected mode, whose current–voltage profile recorded at bus B1 is depicted in Fig. 9. The proposed scheme has been found to be sensitive toward the detection of HIF reliably.

#### 4.6 Real-time validation on OPAL-RT setup

The transient studies on microgrid system models integrated with several DERs and loads involve complex computation with small step size for obtaining higher accuracy. To obtain the results in real time, each submodel is required to be processed simultaneously to avoid the time delay between their executions. So, the performance of the scheme is required to be validated before being used for field

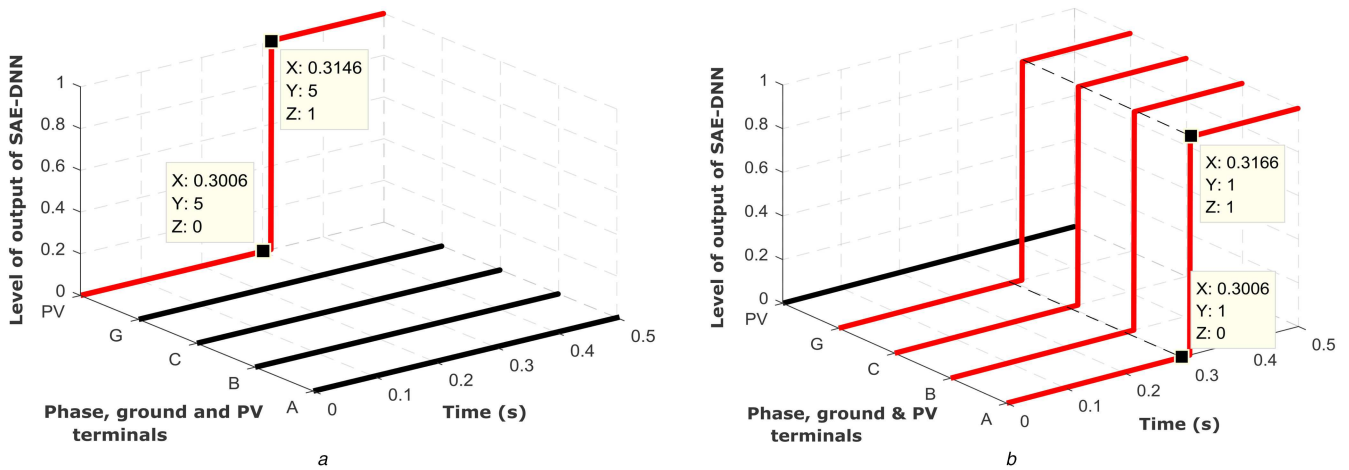


**Fig. 8** Response of the proposed SAE-DNN-based relaying scheme against the fault situations shown in (a) Fig. 2a, (b) Fig. 2b

**Table 5** Response of the proposed SAE-DNN-based protection scheme against high fault resistance ( $R_f$ ) with  $L_f = 10$  km and  $\theta = 45^\circ$

Fault resistance, $\Omega$	Fault type	Faulty section	Grid-connected mode		Islanding mode	
			Fault detector/ classifier output	Relay operation time, s	Fault detector/ classifier output	Relay operation time, s
75	AG	S2	AG	0.0152	AG	0.0159
90	BG	S2	BG	0.0149	BG	0.0164
105	CG	S2	CG	0.0161	CG	0.0162
115	ABG	S2	ABG	0.0153	ABG	0.0159
125	ACG	S4	ACG	0.0158	ACG	0.0161
135	BCG	S4	BCG	0.0163	BCG	0.0165
150	ABCG	S4	ABCG	0.0164	ABCG	0.0158

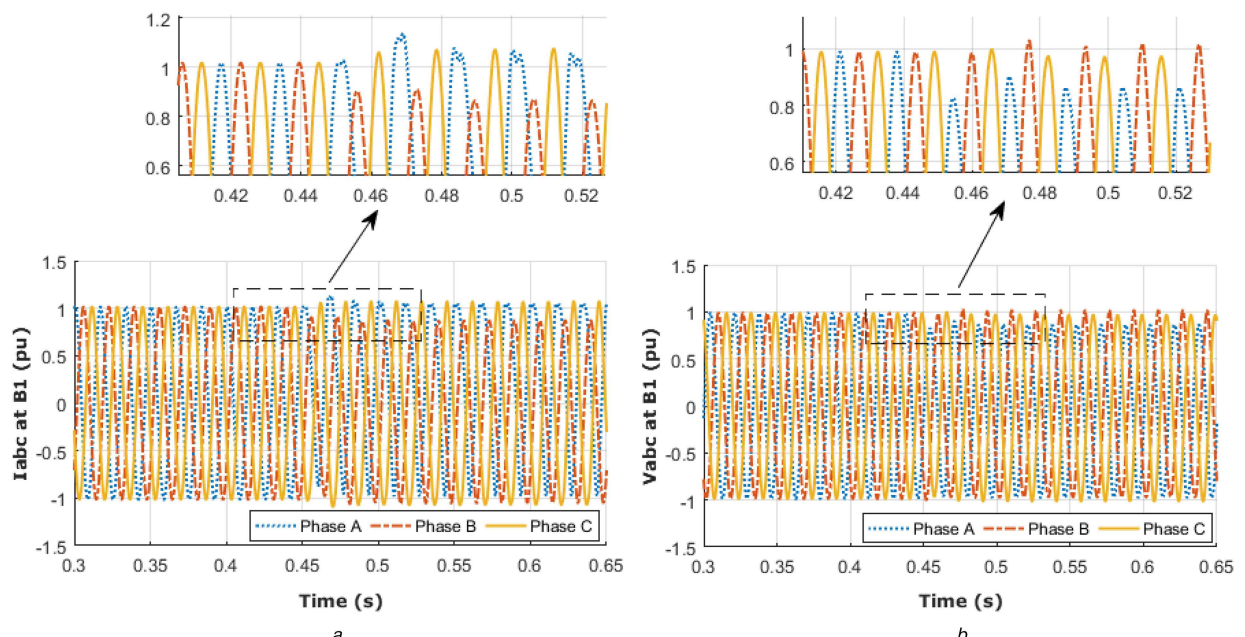


**Fig. 9** Three-phase

(a) Current, (b) Voltage waveform recorded at bus B1 during the inception of high-impedance arc fault in phase A in Section S3 at  $t=0.45$  s with  $L_f=3$  km in the grid-connected mode

applications. In this regard, the developed protection scheme has been implemented on OPAL-RT digital simulator compatible with RT-LAB software providing an interface to a microgrid system model simulated under MATLAB/Simulink environment. The OPAL-RT simulator facilitates parallel processing for fast computation with highly precise simulation results. The experimental setup demonstrating the interconnection of the OPAL-RT digital simulator with host workstation and display unit

is shown in Fig. 10a. To analyse the performance of the proposed scheme on the real-time setting, a random test situation involving ABG fault in Section S3 during islanding mode has been created. The voltage and current signals' pre- and post-fault recorded at bus B1 have been depicted in Figs. 10b and c, respectively. The trip signal was generated by the relay after 14.6 ms of the fault inception as shown in Fig. 10d.

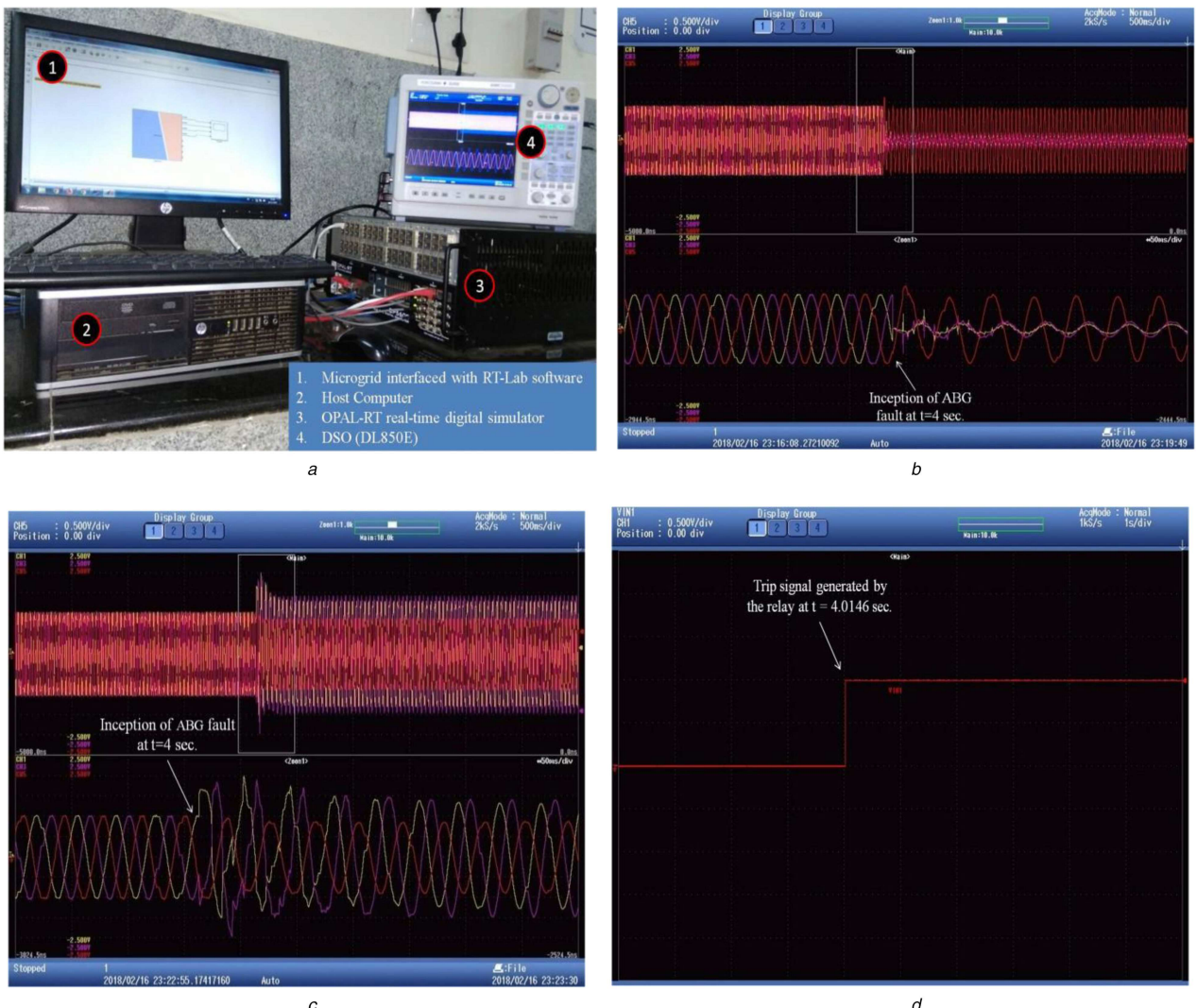


**Fig. 10** Experimental validation of the proposed scheme

(a) OPAL-RT setup, (b) Voltage at bus B1 during ABG fault at  $t = 4$  s, (c) Current at bus B1 during ABG fault at  $t = 4$  s, (d) Trip signal generated by the relay at  $t = 4.0146$  s

A reliable protection scheme should respond fast post-fault. The total time elapsed in the execution of the algorithm, comprising the processing of the time-domain signal, detection and tripping time has been estimated as the relay operation time. The average relay operation time of the proposed SAE-DNN-based scheme has been compared with DT, SVM and ANN-based protection techniques in each mode of microgrid operation in Table 6. The faster response of SAE-DNN-based scheme as compared with the other three techniques ascertains the suitability of the proposed technique for faster restoration post-fault.

## 5 Conclusion

PV integrated microgrids have gained significant importance in recent times due to its ease of operation and economic viability. However, a challenge with regard to the protection of PV integrated microgrids concerns the similar voltage-current profile during PV faults and distribution line faults. The two fault scenarios requiring different relaying actions are not distinguished by conventional protection schemes. In this context, SAE-DNN-based protection scheme has been proposed to address this issue in addition to perform the task of mode detection, fault detection, classification and section identification. The modules for performing the individual tasks have been designed separately for each operating mode of the microgrid. The voltage and current signals recorded at relaying buses are converted into grey-scale images to constitute the dataset for performing the unsupervised feature learning of SAE. Furthermore, the individually trained SAEs are stacked together to form the DNN with softmax classifier. The performance evaluation of the proposed protection

**Table 6** Comparison of the response time of the proposed SAE-DNN scheme with DT, SVM and ANN-based protection techniques

Mode of operation	Technique	Average relay operation time, ms
grid connected	SAE-DNN	13.9
	DT	14.1
	SVM	21.5
	ANN	23.2
islanding	SAE-DNN	15.2
	DT	15.7
	SVM	24.9
	ANN	29.7

scheme has been successfully carried out for diverse operating scenarios of the microgrid involving wide variation in fault parameters. PV array faults (LG and LL) with varying combination are detected and differentiated from symmetrical faults within one cycle. The proposed SAE-DNN-based protection scheme is found to outperform ANN, SVM and DT-based techniques in terms of the reliability indices, i.e. dependability and security under both islanding and grid-connected modes. The scheme has also been validated on the OPAL-RT digital simulator to evaluate its applicability for practical field applications.

## 6 References

- [1] Adefarati, T., Bansal, R.C.: ‘Integration of renewable distributed generators into the distribution system: a review’, *IET Renew. Power Gener.*, 2016, **10**, (7), pp. 873–884
- [2] Xu, X., Mitra, J., Wang, T., *et al.*: ‘An evaluation strategy for microgrid reliability considering the effects of protection system’, *IEEE Trans. Power Deliv.*, 2016, **31**, (5), pp. 1989–1997
- [3] Bacha, S., Picault, D., Burger, B., *et al.*: ‘Photovoltaics in microgrids: an overview of grid integration and energy management aspects’, *IEEE Ind. Electron. Mag.*, 2015, **9**, (1), pp. 33–46
- [4] Mishra, D.P., Samantaray, S.R., Joos, G.: ‘A combined wavelet and data-mining based intelligent protection scheme for microgrid’, *IEEE Trans. Smart Grid*, 2016, **7**, (5), pp. 2295–2304
- [5] Bukhari, S.B.A., Zaman, M.S.U., Haider, R., *et al.*: ‘A protection scheme for microgrid with multiple distributed generations using superimposed reactive energy’, *Int. J. Electr. Power Energy Syst.*, 2017, **92**, pp. 156–166
- [6] Kar, S., Samantaray, S.R.: ‘Time–frequency transform-based differential scheme for microgrid protection’, *IET Gener. Transm. Distrib.*, 2014, **8**, (2), pp. 310–320
- [7] Hooshyar, A., El-Saadany, E.F., Sanaye-Pasand, M.: ‘Fault type classification in microgrids including photovoltaic DGs’, *IEEE Trans. Smart Grid*, 2016, **7**, (5), pp. 2218–2229
- [8] Kumar, D.S., Srinivasan, D., Reindl, T.: ‘A fast and scalable protection scheme for distribution networks with distributed generation’, *IEEE Trans. Power Deliv.*, 2016, **31**, (1), pp. 67–75
- [9] Manohar, M., Koley, E., Ghosh, S.: ‘Reliable protection scheme for PV integrated microgrid using an ensemble classifier approach with real-time validation’, *IET Sci. Meas. Technol.*, 2018, **12**, (2), pp. 200–208
- [10] Oureilidis, K.O., Demoulas, C.S.: ‘A fault clearing method in converter-dominated microgrids with conventional protection means’, *IEEE Trans. Power Electron.*, 2016, **31**, (6), pp. 4628–4640
- [11] Dhar, S., Dash, P.K.: ‘Differential current-based fault protection with adaptive threshold for multiple PV-based DC microgrid’, *IET Renew. Power Gener.*, 2017, **11**, (6), pp. 778–790
- [12] Sabbaghpur Arani, M., Hejazi, M.A.: ‘The comprehensive study of electrical faults in PV arrays’, *J. Electr. Comput. Eng.*, 2016, **2016**
- [13] Alam, M.K., Khan, F., Johnson, J., *et al.*: ‘A comprehensive review of catastrophic faults in PV arrays: types, detection, and mitigation techniques’, *IEEE J. Photovoltaics*, 2015, **5**, (3), pp. 982–997
- [14] Zhao, Y., De Palma, J.F., Mosesian, J., *et al.*: ‘Line–line fault analysis and protection challenges in solar photovoltaic arrays’, *IEEE Trans. Ind. Electron.*, 2013, **60**, (9), pp. 3784–3795
- [15] Ray, P., Mishra, D.P.: ‘Support vector machine based fault classification and location of a long transmission line’, *Eng. Sci. Technol., Int. J.*, 2016, **19**, (3), pp. 1368–1380
- [16] Kar, S.: ‘A comprehensive protection scheme for micro-grid using fuzzy rule base approach’, *Energy Syst.*, 2017, **8**, (3), pp. 449–464
- [17] Kar, S., Samantaray, S.R., Zadeh, M.D.: ‘Data-mining model based intelligent differential microgrid protection scheme’, *IEEE Syst. J.*, 2017, **11**, (2), pp. 1161–1169
- [18] Gururani, A., Mohanty, S.R., Mohanta, J.C.: ‘Microgrid protection using Hilbert–Huang transform based-differential scheme’, *IET Gener. Transm. Distrib.*, 2016, **10**, (15), pp. 3707–3716
- [19] Chen, K., Hu, J., He, J.: ‘A framework for automatically extracting overvoltage features based on sparse autoencoder’, *IEEE Trans. Smart Grid*, 2018, **9**, (2), pp. 594–604
- [20] Xia, M., Li, T., Liu, L., *et al.*: ‘Intelligent fault diagnosis approach with unsupervised feature learning by stacked denoising autoencoder’, *IET Sci. Meas. Technol.*, 2017, **11**, (6), pp. 687–695
- [21] Qi, Y., Shen, C., Wang, D., *et al.*: ‘Stacked sparse autoencoder-based deep network for fault diagnosis of rotating machinery’, *IEEE Access*, 2017, **5**, pp. 15066–15079
- [22] Geng, J., Fan, J., Wang, H., *et al.*: ‘High-resolution SAR image classification via deep convolutional autoencoders’, *IEEE Geosci. Remote Sens. Lett.*, 2015, **12**, (11), pp. 2351–2355
- [23] Sun, W., Shao, S., Zhao, R., *et al.*: ‘A sparse auto-encoder-based deep neural network approach for induction motor faults classification’, *Measurement*, 2016, **89**, pp. 171–178
- [24] Kumar, B.P., Ilango, G.S., Reddy, M.J.B., *et al.*: ‘Online fault detection and diagnosis in photovoltaic systems using wavelet packets’, *IEEE J. Photovoltaics*, 2018, **8**, (1), pp. 257–265
- [25] Shin, H.C., Orton, M.R., Collins, D.J., *et al.*: ‘Stacked autoencoders for unsupervised feature learning and multiple organ detection in a pilot study using 4D patient data’, *IEEE Trans. Pattern Anal. Mach. Intell.*, 2013, **35**, (8), pp. 1930–1943
- [26] Hosseini-Asl, E., Zurada, J.M., Nasraoui, O.: ‘Deep learning of part-based representation of data using sparse autoencoders with nonnegativity constraints’, *IEEE Trans. Neural Netw. Learn. Syst.*, 2016, **27**, (12), pp. 2486–2498
- [27] Gautam, S., Brahma, S.M.: ‘Detection of high impedance fault in power distribution systems using mathematical morphology’, *IEEE Trans. Power Syst.*, 2013, **28**, (2), pp. 1226–1234